

Scaling laws for the high-pressure inductively coupled plasma torch under thermochemical non-equilibrium

D. Vanden-Abee^{a,b,*}, G. Degrez^{a,b}

^aUniversité Libre de Bruxelles, Service de Mécanique des Fluides, 50 Av. F.D. Roosevelt, Brussels, B-1050, Belgium

^bVon Karman Institute for Fluid Dynamics, Department of Aeronautics and Aerospace, 72 Stwg-op-Waterloo, St. Genesius-Rode, B-1640, Belgium

Abstract

We have recently derived a useful set of scaling laws for the operating parameters of the high-pressure inductively coupled plasma torch and have verified the validity of our results by performing numerical simulations of inductively coupled plasmas of varying diameters, assuming local thermodynamic equilibrium conditions. In this contribution, we present complementary non-equilibrium simulations to demonstrate that our scaling laws hold even when departures from equilibrium are important.

Keywords: Inductively coupled plasma (ICP) torch; Magneto-hydrodynamics (MHD); Numerical simulation; Modeling

1. Introduction

To efficiently produce stable inductively coupled plasmas (ICPs), it is essential that the four operating parameters of an ICP torch (generator frequency f , power dissipated into the plasma \dot{W} , mass flow rate \dot{m} and operating pressure p_0) be well adapted to its dimensions. To better understand this relationship, we have recently derived a dimensionless form of the equations governing the behavior of such plasmas. It has been shown that the requirement of similarity naturally leads to useful expressions for the operating parameters as a function of the radius R of the plasma torch [1]:

$$f \propto R^{-2}; \dot{W} \propto R; \dot{m} \propto R; p_0 \propto R^{-2} \quad (1)$$

Herein, the scaling law for pressure must be respected only when the magnetic interaction parameter I (= the ratio of Lorentz forces to inertia) is of order one or greater. We have also provided an approximate expression $I = \alpha(p_0 \dot{W} R) / (f \dot{m}^2)$, where, for air and argon ICPs, $\alpha \approx 0.15 \text{ MHz (g/s)}^2 (\text{bar W cm})^{-1}$.

The above results were derived under the assumption that the plasma is under local thermodynamic equilibrium (LTE) and have been supported by LTE

calculations of ICP torches of varying diameters. The extension of the analysis to the more general case where thermal and chemical non-equilibrium effects are important suggests that similarity may still be maintained provided a slightly weaker scaling $p_0 \propto R^{-1}$ is used for pressure [1]. The most general form for the scaling laws, valid even under non-equilibrium, then reads:

$$f \propto R^{-2}; \dot{W} \propto R; \dot{m} \propto R; p_0 \propto R^{-1}; I < 1 \quad (2)$$

In this contribution, we present numerical simulations of air ICPs under thermal and chemical non-equilibrium to demonstrate the correctness of the above correlations.

2. Governing equations

For completeness, we here include a brief overview of the numerical model used for the simulations; for the full details, the reader is referred to [2,3].

2.1. Axisymmetric representation of the ICP torch

An ICP torch essentially consists of a quartz tube, surrounded by a thick copper inductor. A powerful radio-frequency electric current (of amplitude I_c and

*Corresponding author. Tel.: +32 2 650 26 90; Fax: +32 2 650 27 10; E-mail: David.Vanden.Abee@ulb.ac.be

frequency f) oscillates through the inductor and induces a secondary current inside the tube. The gas flowing through the tube is heated to a plasma state with peak temperatures $\sim 10\,000$ K through Ohmic dissipation. For reasons of flow stability, the injection of gas is done in an annular, swirling manner close to the tube wall.

We can model the torch by a fully axisymmetric configuration by approximating the (solenoidal) inductor by a series of n_c parallel, current-carrying rings. For simplicity, we assume the rings to be infinitely thin current loops, located at the innermost part of the true coil rings, where most of the electric current is known to run. The axisymmetric ICP geometry used for the present simulations is shown on Fig. 1.

2.2. MHD induction equation

The induced electric field \vec{E} is purely toroidal and consists of a single Fourier mode at the torch operating frequency: $\vec{E} = E \exp(i2\pi ft) \vec{e}_\theta$. It can be shown to satisfy the following Helmholtz-type MHD induction equation, both inside the torch and on a far field domain covering the space around the torch [2]:

$$\frac{\partial^2 E}{\partial z^2} + \frac{1}{r} \frac{\partial}{\partial r} \left(r \frac{\partial E}{\partial r} \right) - \frac{1}{r^2} E - i\mu_0 2\pi f \sigma E = -i\mu_0 2\pi f J_{\text{Ext}} \quad (3)$$

where the right-hand side represents the effect of the singular external current density in the n_c rings with position \vec{r}_c : $J_{\text{Ext}} = I_c \sum_{c=1}^{n_c} \delta(\vec{r} - \vec{r}_c)$.

2.3. Flow field equations

The radio-frequency electro-magnetic field generates small oscillating perturbations on all flow field quantities. By averaging the flow equations in time, a quasi-steady flow field formulation similar to the steady Navier-Stokes equations is obtained. In the momentum equation, a time-averaged Lorentz force \vec{F}_L appears; in the energy equation(s), a time-averaged Joule heating source term P_J must be included.

Given the rapid energy exchange between free and bound electronic states and the vibrational states of N_2 [4] (the main molecular species in air ICPs), we suppose that these energies are mutually equilibrated at a common electro-vibrational temperature T_{ev} . On the other hand, the translational and rotational energies of heavy particles are considered to share a common translational-rotational temperature T_{tr} . The following set of flow field equations is then solved (in axisymmetric coordinates) [2]:

$$\nabla \cdot (\rho \vec{u}) = 0 \quad (4)$$

$$\nabla \cdot (\rho \vec{u} y_s) + \nabla \cdot \vec{J}_s = \omega_s \quad (5)$$

$$\nabla \cdot (\rho \vec{u} : \vec{u} + \hat{p} - \hat{\tau}) = \vec{F}_L \quad (6)$$

$$\nabla \cdot (\rho \vec{u} h) + \nabla \cdot \left(\sum_{s=1}^{nsp} \vec{J}_s h_s \right) = \nabla \cdot (\Lambda_{hr} \nabla T_{hr}) + \nabla \cdot (\Lambda_{ev} \nabla T_{ev}) + P_J \quad (7)$$

$$\nabla \cdot (\rho \vec{u} h_{ev}) + \nabla \cdot \left(\sum_{s=1}^{nsp} \vec{J}_s h_{s,ev} \right) = \nabla \cdot (\Lambda_{ev} \nabla T_{ev}) + \frac{\rho e_{ev}(T_{ev} - e_{ev}(T_{hr}))}{\tau_{ev}} + P_{\text{Chem}} + P_J \quad (8)$$

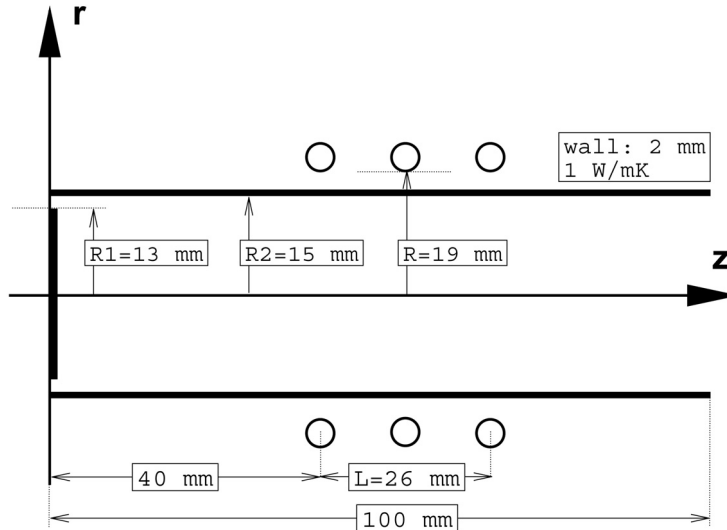


Fig. 1. Torch geometry used for the simulations at scaling factor 1.

Herein, \vec{J}_s represents the mass diffusive flux of a species s and the production/destruction of this species due to finite-rate chemistry is written ω_s . Λ_{hr} and Λ_{ev} stand for the combined thermal conductivity of heavy particle translational and rotational modes, respectively, the electron, electronic and vibrational modes. In the electro-vibrational energy equation, τ_{ev} stands for the mutual relaxation time of electro-vibrational and translation-rotational energies due to elastic and inelastic collisions. The electro-vibrational energy loss due to chemical reactions is written P_{Chem} .

All details concerning the modeling of thermodynamic, transport, and chemical properties in the above equations have been discussed in detail in [2,3]. The finite-rate chemistry model used is the one by Park, as listed by Gnoffo et al. [4].

3. Operating conditions for the numerical simulations

Simulations are performed for the geometry shown in Fig. 1 at a scaling factor of 1 and 3, using the following operation conditions:

- $f = 27$ MHz, $\dot{W} = 3$ kW, $\dot{m} = 0.5$ g/s, $p_0 = 0.1$ bar.
- $f = 3$ MHz, $\dot{W} = 9$ kW, $\dot{m} = 1.5$ g/s, $p_0 = 0.333$ bar.

One may readily verify that these conditions respect Eqs. (2) and that $I < 1$ indeed. The governing equations are discretized using a second-order accurate cell-centered finite-volume discretization and are solved using a damped Newton method on a stretched mesh of 50 by 25 cells.

4. Analysis and conclusion

In Figs 2, 3 and 4, we compare solution fields for the translational-rotational and electro-vibrational temperatures and for the mole fraction of electrons. All results shown are at least six orders of magnitude converged. The agreement between the original ICP torch and its scaled-up version is found to be excellent. This is remarkable, given the fact that we are dealing with a complex non-equilibrium flow. We hope that the scaling laws included in this paper will be put into practical use and are eager to receive feedback from experimentalists in the field.

References

- [1] Vanden-Abee D, Degrez G. Similarity analysis for the high-pressure inductively coupled plasma source. *Plasma Sources, Science and Technology* 2004;13:680–690.
- [2] Vanden-Abee D, Degrez G. Numerical model of high-pressure air inductive plasmas under thermal and chemical non-equilibrium. *AIAA Technical Paper* 2000–2416; 31st AIAA Plasmadynamics and Lasers Conference, Denver, Colorado, 2000.
- [3] Bottin B, Vanden-Abee D, Carbonaro M, Degrez G, Sarma, GSR. Thermodynamic and transport properties for induction plasma modeling. *J of Thermophysics and Heat Transfer* 1999;13(3):343–350.
- [4] Gnoffo PA, Gupta, RN, Shinn, JL. Conservation equations and physical models for hypersonic air flows in thermal and chemical non-equilibrium. *NASA Technical Paper* 2867; NASA, Hampton, Virginia, 1989.

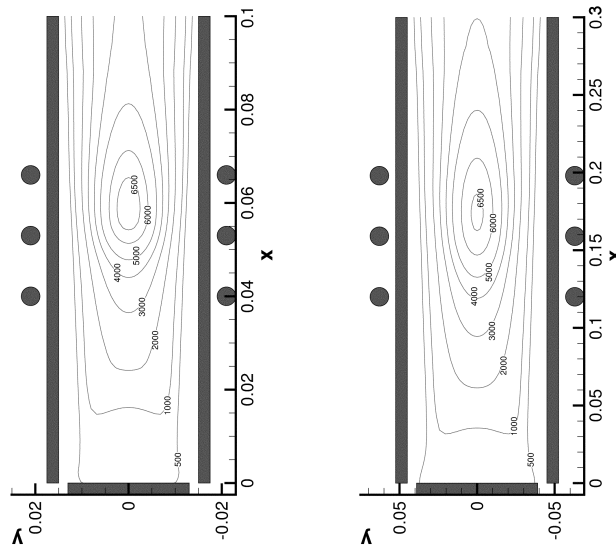


Fig. 2. Comparison of heavy particle temperature fields computed for a scaling factor of 1 (left) and 3 (right).

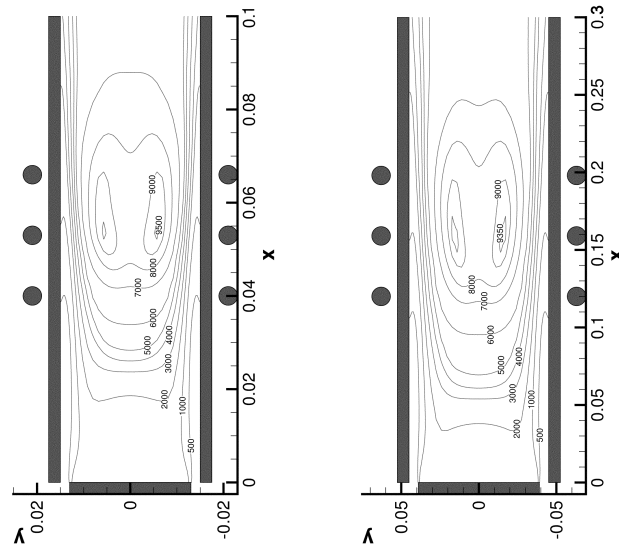


Fig. 3. Comparison of electro-vibrational temperature fields computed for a scaling factor of 1 (left) and 3 (right).

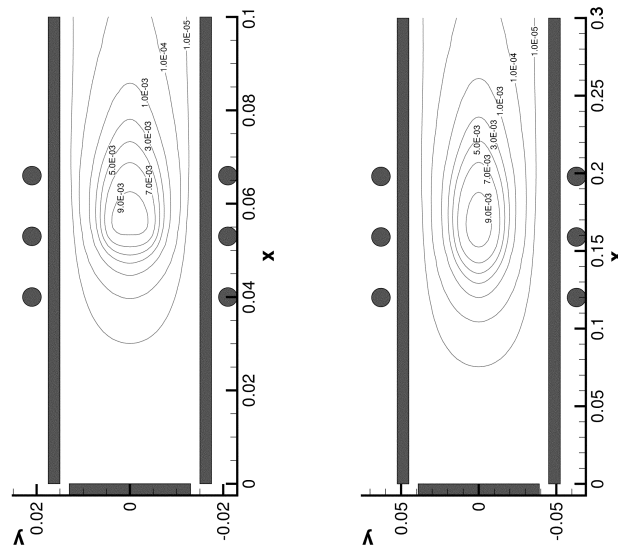


Fig. 4. Comparison of electron concentration fields computed for a scaling factor of 1 (left) and 3 (right).